Neurochemistry International 129 (2019) 104508

Contents lists available at ScienceDirect

Neurochemistry International

journal homepage: www.elsevier.com/locate/neuint

Glutaminase activity in GLS1 Het mouse brain compared to putative pharmacological inhibition by ebselen using *ex vivo* MRS

Lauren Kosten[a], Golam M.I. Chowdhury[b], Susana Mingote[c,d,f], Steven Staelens[a], Douglas L. Rothman[e], Kevin L. Behar[b,**], Stephen Rayport[c,d,*]

[a] Molecular Imaging Center Antwerp, University of Antwerp, Antwerp, Belgium
[b] Department of Psychiatry, Magnetic Resonance Research Center, Yale University School of Medicine, USA
[c] Department of Psychiatry, Columbia University, USA
[d] Department of Molecular Therapeutics, NYS Psychiatric Institute, USA
[e] Department of Radiology & Biomedical Imaging, Magnetic Resonance Research Center, Yale University School of Medicine, USA
[f] Neuroscience, Advanced Science Research Center at the Graduate Center of the City University of New York, USA

ARTICLE INFO

Keywords:
Magnetic resonance spectroscopy
Focused beam microwave irradiation
Glutamate-glutamine cycling
GABA
Schizophrenia pharmacotherapy

ABSTRACT

Glutaminase mediates the recycling of neurotransmitter glutamate, supporting most excitatory neurotransmission in the mammalian central nervous system. A constitutive heterozygous reduction in GLS1 engenders in mice a model of schizophrenia resilience and associated increases in Gln, reductions in Glu and activity-dependent attenuation of excitatory synaptic transmission. Hippocampal brain slices from GLS1 heterozygous mice metabolize less Gln to Glu. Whether glutaminase activity is diminished in the intact brain in GLS1 heterozygous mice has not been assessed, nor the regional impact. Moreover, it is not known whether pharmacological inhibition would mimic the genetic reduction. We addressed this using magnetic resonance spectroscopy to assess amino acid content and ^{13}C-acetate loading to assess glutaminase activity, in multiple brain regions. Glutaminase activity was reduced significantly in the hippocampus of GLS1 heterozygous mice, while acute treatment with the putative glutaminase inhibitor ebselen did not impact glutaminase activity, but did significantly increase GABA. This approach identifies a molecular imaging strategy for testing target engagement by comparing genetic and pharmacological inhibition, across brain regions.

1. Introduction

Glutaminase (GLS) mediates the conversion of glutamine (Gln) to glutamate (Glu), supporting most excitatory neurotransmission in the mammalian central nervous system (CNS) (Hertz, 2004; Marx et al., 2015; Sibson et al., 1997). There are two genes encoding GLS, also called phosphate-activated glutaminase. *Gls1* codes for the brain-kidney isoform, and *Gls2* for the liver isoform. GLS has a crucial role in brain function, as mice lacking *Gls1* manifest behavioral and respiratory problems, and die within the first day of life (Masson et al., 2006); similarly, human infants with loss of *GLS* function manifest encephalopathy, status epilepticus, and early demise (Rumping et al., 2018). In contrast, *Gls1* heterozygous (GLS1 Het) mice are phenotypically quite normal, with subtle phenotypes associated with schizophrenia resilience, including diminished sensitivity to propsychotic challenge (Gaisler-Salomon et al., 2009a). Resilience models point to potential novel therapeutic targets for the pharmacotherapy of psychiatric disorders, such as schizophrenia (Mihali et al., 2012).

In GLS1 Hets, Glu content in brain tissue is reduced by about 15% and GLS activity 50%, (Gaisler-Salomon et al., 2009a). However, the reduced activity mainly reflects reduction in GLS protein, and not the actual activity of GLS in the brain, which is subject to multiple modes of regulation (Curthoys and Watford, 1995). Metabolic flux through GLS in *ex vivo* brain slices is reduced by about 20% in GLS1 Hets, measured with ^{13}C-Gln and MRS (El Hage et al., 2012). Whether GLS function is diminished in the intact brain of GLS1 Het mice, and whether there are

Abbreviations: CB, cerebellum; CNS, central nervous system; FBMI, focused-beam microwave irradiation; GABA, gamma-aminobutyric acid; GAD, glutamic acid decarboxylase; GDH, glutamate dehydrogenase; Gln, glutamine; GLS, glutaminase; Glu, glutamate; GPx, glutathione peroxidase; Het, heterozygous; HIP, hippocampus; i.p, intraperitoneal; MRS, magnetic resonance spectroscopy; NMDA, N-methyl-D-aspartate; PFC, prefrontal cortex; STR, striatum; THA, thalamus; WT, Wildtype

* Corresponding author. Department of Psychiatry, Columbia University, USA.
** Corresponding author.
E-mail addresses: Kevin.behar@yale.edu (K.L. Behar), stephen.rayport@nyspi.columbia.edu (S. Rayport).

https://doi.org/10.1016/j.neuint.2019.104508
Received 17 May 2019; Received in revised form 28 June 2019; Accepted 18 July 2019
Available online 19 July 2019
0197-0186/

regional differences has not been determined. Furthermore, it is not known whether the pharmacological inhibition of GLS would mimic the genetic reduction.

While there are several recognized GLS inhibitors (*e.g.,* DON, BPTES, C968, CB-839), they have millimolar to micromolar-range K_i's or do not permeate the blood brain barrier. In contrast, ebselen, which was developed as a glutathione peroxidase (GPx) mimic, permeates the blood brain barrier (Azad et al., 2014; Sies, 1993), and was recently reported to be a potent allosteric GLS inhibitor with a low-nanomolar K_i (Thomas et al., 2013), and a two-fold greater activity against GLS than other most potent reported activities (Thomas et al., 2013). As in the GLS1 Het mice and adult-induced GLS1 Het mice (Mingote et al., 2016), ebselen attenuates amphetamine-induced hyperlocomotion (Singh et al., 2013). Ebselen treatment phenocopies the schizophrenia resilience phenotype of GLS1 Het mice with both antipsychotic and pro-cognitive effects, seen in attenuation of amphetamine sensitization and enhanced social recognition, respectively (Heffetz-Giterman et al., 2018). In a recent MRS study in humans, ebselen reduced cortical Glu and Gln levels (4–6%), measured by ^{1}H MRS at 7T (Masaki et al., 2016), pointing to GLS-based action. Ebselen has also been shown to rescue prepulse inhibition (PPI) deficits in the neonatal ventral hippocampal lesion rodent schizophrenia model (Cabungcal et al., 2014).

Given the multiple mechanisms of action of ebselen, relating its potential therapeutic effects to a particular mechanism of action *in vivo* is challenging, in particular its probable action as a GLS inhibitor. Indeed, a more recent study by Zhu et al. (2017) showed that ebselen is only a micromolar GLS inhibitor (10% inhibition at 10 μM), and instead a potent glutamate dehydrogenase (GDH) inhibitor (K_i, 300 nM). The apparent nanomolar GLS inhibition was likely due to inhibition of the downstream enzymes used in the assay. Higher doses of ebselen (10 mg/kg), leading to a body concentration of 50 μM, which we test in this study, might nonetheless inhibit GLS to some extent.

To compare the impact of the genetic heterozygous reduction in *Gls1* to putative pharmacological inhibition with ebselen, we used ^{1}H-[^{13}C] MRS to measure regional Gln, Glu and associated metabolites, and the flux from Gln to Glu following [2–^{13}C]acetate infusion, in the intact brain. Acetate labeled with 13C is taken up exclusively by astrocytes and metabolized in the tricarboxylic acid cycle, labeling Gln (Patel et al., 2010). Gln is released from astrocytes to neurons where it is catalyzed by GLS to Glu. Kinetic analysis shows that the ratio of ^{13}C-Glu to ^{13}C-Gln at 15 min of infusion reflects GLS activity. We also measured GABA because of its dependence on Glu as a precursor. We found that GLS activity is modestly reduced in GLS1 Hets, principally in hippocampus, while ebselen had no effect.

2. Materials and methods

2.1. Animals

Mice were handled in accordance with the guidelines of the National Institutes of Health Guide for the Care and Use of Laboratory Animals, under protocols approved by the Institutional Animal Care and Use Committees of New York State Psychiatric Institute and Yale University. All efforts were made to minimize animal suffering according to the Animal Welfare Act (7 USC 2131).

GLS1 Het mice were originally developed as stopGLS1 mice with a transcriptional block of *Gls1* expression (Masson et al., 2006). The same upstream region of exon 1 was floxed and deleted to produce deltaGLS1 mice (Mingote et al., 2016), which were used in this study. Eighteen animals ages 73–89 days were tested, with a total of 10 males and 8 females, subdivided in WT (n = 6, 2 males and 4 females), GLS1 Het (n = 7, 5 males and 2 females) and ebselen-treated WT (n = 5, 3 males and 2 females) cohorts, weighing 21 ± 2, 23 ± 3 and 23 ± 2 g, respectively.

GLS1 Het mice were bred with WT mice to generate GLS1 Het and WT littermate controls at NYSPI, under IACUC protocol 1428. Mice were 50:50 C57BL/6J:129J background. Mice were transferred to Yale, and experiments conducted under IACUC protocol 2015–11495. Mice were prepared 7 days before infusion with jugular vein catheters inserted under isoflurane anesthesia (2–3%; 28% O_2/70% N_2O). Meloxicam (0.03–0.05 mg/kg, s.c., daily for 3 days post-surgery) was administered for analgesia. Ebselen 10 mg/kg (Hello Bio, Princeton, NJ, USA) was administered by intraperitoneal injection (Singh et al., 2013) 30 min prior to ^{13}C-acetate infusion. Higher doses of ebselen (30 mg/kg) were avoided due to detrimental effects on nerve conduction in rats (Ozyigit et al., 2015).

2.2. ^{13}C-acetate infusion and Focused-Beam Microwave Irradiation

On the day of the study, the jugular vein catheter was quickly freed from the subcutaneous pouch under brief isoflurane anesthesia. Mice were allowed to recover for at least 30 min, once awake and behaving freely, they then received timed infusions of [2–^{13}C]-acetate (in water, 2 mol/L, pH 7; 15 min), with an initial 15 s bolus followed by step-down infusion (in μmol/min/g body weight: 0–15 s, 4.68; 15 s to 4 min, 0.648; 4 min–15 min, 0.375) based on previous kinetic analyses of acetate transport and metabolic rates (Patel et al., 2010). After the infusion, mice were quickly sedated (< 30 s) with isoflurane and euthanized by Focused-Beam Microwave Irradiation (FBMI; 0.62 s, 4.5 kW, Model TMW-4012C-10 kW, Muromachi Kikai Co., Ltd., Tokyo, Japan), which halts cerebral metabolism by rapid heat-inactivation of enzymes (de Graaf et al., 2009). The brain was rapidly removed, the regions of interest dissected (prefrontal cortex PFC; hippocampus HIP; thalamus THA; striatum STR and cerebellum CB), frozen in liquid N_2 and stored at −80 °C. Heart blood was sampled postmortem for measurement of infused acetate concentration and ^{13}C-enrichment.

2.3. Brain tissue extraction

Frozen brain tissue was homogenized using a bead mill homogenizer (1.4 mm ceramic beads; Omni Bead Ruptor 24, Omni International, Kennesaw, GA) with methanol in 0.1 M HCl (2:1 vol/wt), followed by 90% ethanol in 0.1 M phosphate buffer (pH 7; 6:1 vol/wt) and ultrapure water (8:1 vol/wt), with homogenization in between. [2–^{13}C]-Glycine was added at the first step as an internal concentration reference. After centrifugation, the supernatant was saved, and the pellet re-homogenized in 60% ethanol. Following centrifugation, the supernatants were combined and eluted through a Chelex-100 resin-packed column. Eluted samples were titrated to pH 7 with NaOH, lyophilized and resuspended in 500 μl of a solution containing 3-trimethylsilyl-[2,2,3,3-D_4]-propionate (TSP, 0.25 mM), 50 mM PO_4^{-3} (pH 7) and 80% D_2O/20% H_2O v/v. for MRS analysis at 11.7 T using ^{1}H-[^{13}C]-NMR. All solutions were prepared using Type 1 ultrapure water (Milli-Q Integral 10, Millipore Sigma, Burlington, MA USA).

2.4. Magnetic resonance spectroscopy

Fully relaxed ^{1}H-[^{13}C] MRS spectra were acquired as two subspectra at 11.7 T (^{1}H resonance frequency of 500.13 MHz) using a Bruker AVANCE spectrometer (Bruker Instruments, Billerica, MA, USA) – one involving broadband ^{13}C inversion pulses applied in alternate scan blocks, while ^{13}C-decoupling was applied in both. Subtraction of the scans obtained with ^{13}C inversion (^{12}C-^{13}C) from those without inversion (^{12}C + ^{13}C) resulted in a difference spectrum containing only ^{13}C coupled ^{1}H resonances at twice the true intensity (2 × ^{13}C).

Quantification of amino acids in the ^{1}H-[^{13}C]NMR spectra of brain extracts was performed by integration of the specified proton resonances (e.g., glutamate H4, GABA H2, etc.) over a fixed chemical shift range free of overlap and corrected for finite bandwidth by dividing by the integral fraction determined previously for the pure compounds. ^{13}C per cent enrichment was calculated as the ratio, [^{13}C/(^{12}C + ^{13}C)]

× 100, followed by subtraction of 1.1% to remove ^{13}C arising from natural abundance. Absolute concentrations of metabolites in brain extracts were determined from the total (^{12}C + ^{13}C) spectrum relative to the [2–^{13}C]-glycine standard in the difference spectrum. The isotopic ^{13}C enrichments of glutamate (Glu)-C4, GABA-C2, and glutamine (Gln)-C4 were calculated from the ratio of the areas of these resonances in the ^{1}H-[^{13}C]-NMR difference spectrum (2 × ^{13}C only) and the non-edited spectrum ($^{12}C+^{13}C$). The isotopic ^{13}C enrichment of acetate-C2 (1.9 ppm) in blood plasma was calculated by dividing the areas of the ^{13}C satellites with the total area ($^{12}C+^{13}C$) of their respective resonances (Chowdhury et al., 2007).

2.5. Statistical analyses

Statistical significance was determined using the Kruskal-Wallis test for overall treatment effects and Mann-Whitney *U* test with Bonferroni correction for multiple comparisons to analyze significant interactions, using IBM SPSS Statistics 25.0 (IBM, Armonk, NY). Each region was analyzed individually, without assuming a consistent SD. Effects were considered significant for p-values ≤ 0.05. Some samples were lost during processing, resulting in a slightly smaller sample size of n = 4 for WT and n = 4 for ebselen-treated cohort in hippocampus. All data were expressed as mean ± SEM; the SD's are given in supplemental tables. Outlier analysis was performed with an *a*bsolute *d*eviation from the *m*edian (MAD) criterion defined as $M-3^{*}MAD < x_i < M+3^{*}MAD$ (Leys et al., 2013), resulting in the exclusion of 11 outlier data points over all measurements. For the comparison of effect sizes to the previous *in vitro* MRS study (El Hage et al., 2012), we used Cohen's d, since El Hage et al., 2012 did a parametric analysis.

3. Results

3.1. Blood-plasma ^{13}C acetate enrichment

To avoid anesthesia effects on cerebral metabolic rates and examine the regional impact of GLS reduction or inhibition in mouse brain, we used *ex vivo* MRS. Three groups of mice were studied: wildtype, GLS1 Het and ebselen-treated. ^{13}C-acetate was infused intravenously for 15 min in awake, freely behaving mice, and then metabolism rapidly arrested by FBMI. The ^{13}C enrichment of blood plasma acetate-C2 did not differ between groups: control (81.78 ± 7.08%, n = 6), GLS1 HET (77.35 ± 6.55%, n = 7) and ebselen-treated (85.08 ± 6.56%, n = 5) mice (p = 0.14).

3.2. Amino acid content

We measured total amino acid content of both ^{13}C-labeled and unlabeled isotopomers from the ^{1}H-[^{13}C] MRS spectra. Fig. 1 shows representative sample spectra for PFC, the first anatomical region sampled. Summary data are shown in Fig. 2 and the full data set in Supplemental Table for Fig. 2. GLS1 Hets showed no significant differences, although slightly lower levels of Glu were seen in CB and STR and GABA in CB and THA; slightly higher levels of Glu were seen in PFC, and Gln in HIP and PFC. Ebselen-treated mice showed no significant differences, although slightly higher levels of Glu were seen in PFC, and GABA in HIP and PFC. Ebselen-treated mice differed from GLS1 Hets, in showing significant increases in Glu in STR (p = 0.03) and GABA in HIP (p = 0.036).

3.3. Metabolic labeling

We then measured ^{13}C enrichment of amino acids (Fig. 3 and Supplemental Table for Fig. 3). Gln-C4 was greater than Glu-C4 and GABA-C2 in all mice, for all regions, as expected for metabolism of this astrocyte-selective substrate. Glu-C4, Gln-C4 and GABA-C2 appeared lower in GLS1 Hets in PFC but not other regions, although not statistically significant. The average Gln-C4 enrichment appeared slightly higher in THA compared to WT. In ebselen-treated mice, average enrichments appeared higher than GLS1 Hets for Glu-C4 in all regions, particularly in HIP and THA, although not statistically significant.

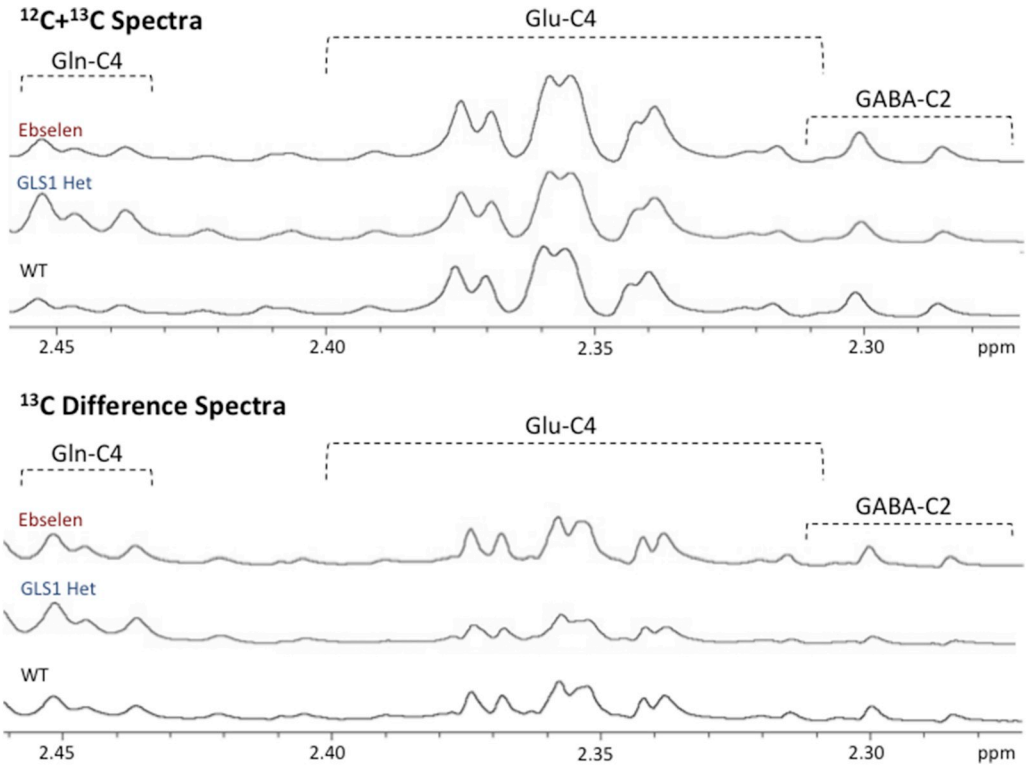

Fig. 1. Representative *ex vivo* spectra in PFC samples from WT, GLS1 Het and ebselen-treated mice. The top panel shows ^{1}H-[^{13}C] MRS spectra, for total content. The bottom panel shows ^{1}H-[^{13}C] MRS containing only ^{13}C coupled ^{1}H resonances, at twice the true intensity for ^{13}C labeled metabolites. Spectra were acquired at 11.7 T with a ^{1}H resonance frequency of 500.13 MHz. The GLS1 Het spectra show higher Gln-C4 concentration (top panel) and lower Glu-C4 labeling (bottom panel), compared to WT.

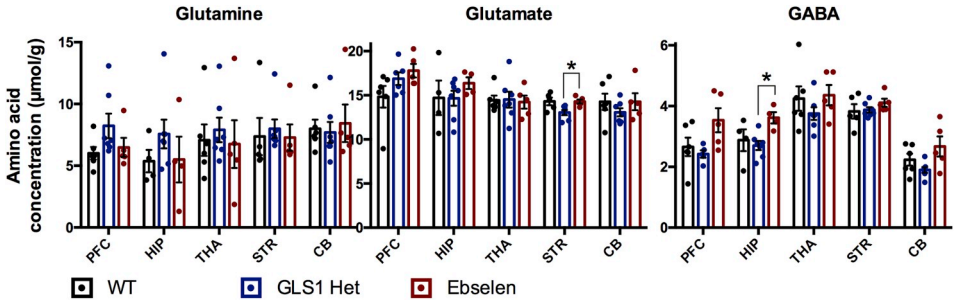

Fig. 2. Amino acid content measured from ^{1}H-[^{13}C] MRS spectra. Regional comparison of glutamine, glutamate and GABA content in GLS1 Het mice with a genetic reduction of GLS or wild type (WT) mice following putative pharmacologic GLS inhibition, compared to WT. Mice had undergone 15 min [2–^{13}C]-acetate infusions, but here the ^{1}H signals were used to determine total content. Values are given in Supplemental Table for Fig. 2. In this and subsequent figures, all data points are plotted, with bars showing mean ± SEM. *p < 0.05.

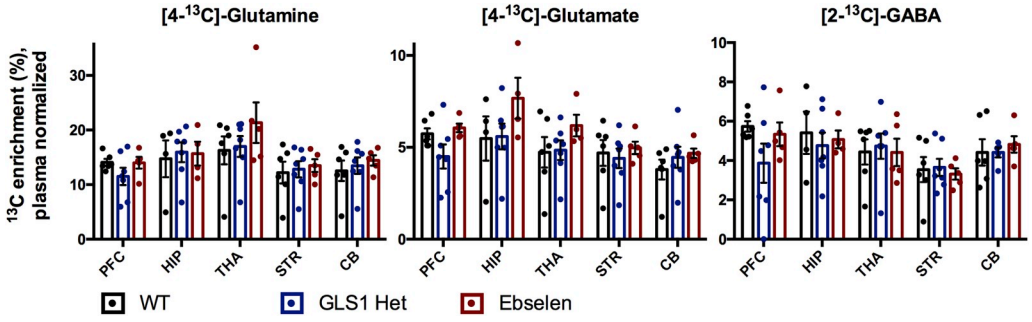

Fig. 3. Regional comparison of ^{13}C enrichment in glutamine (Gln-C4), glutamate (Glu-C4) and GABA (GABA-C2) versus plasma, following 15 min [2–^{13}C]-acetate infusion. Values are ^{13}C enrichment above the 1.1% natural abundance, relative to plasma [2–^{13}C]-acetate enrichment. ^{13}C labeled Gln was significantly greater than Glu or GABA, consistent with initial metabolism of ^{13}C acetate to Gln in astrocytes. Values are given in Supplemental Table for Fig. 3.

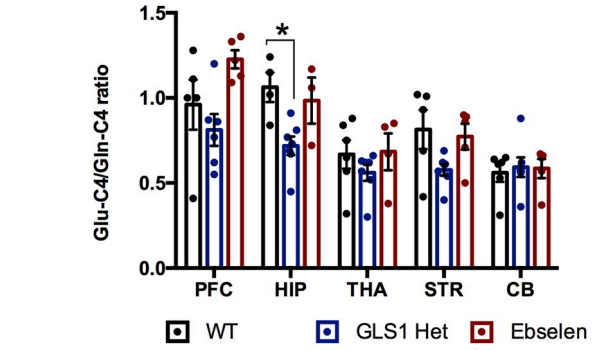

Fig. 4. Regional comparison in the ^{13}C-labeled Glu-C4/Gln-C4 ratio, following 15 min [2–^{13}C]-acetate infusion, as an index of GLS activity. GLS activity was significantly reduced in the HIP of GLS1 Hets, and trended lower in all other regions, except CB. *p < 0.05.

3.4. Glutaminase activity

GLS activity was measured as the ratio of [2–^{13}C]-acetate labeled Glu-C4 to Gln-C4, after 15 min infusion of ^{13}C-acetate (Fig. 4 and Supplemental Table for Fig. 4). The Glu-C4/Gln-C4 ratio was significantly lower in the HIP in GLS1 Hets ($p = 0.036$). The ratio appeared lower in THA, PFC and STR, although not statistically significant, while there was no difference in CB. There were no significant differences in ebselen-treated mice. Compared to GLS1 Hets, there was a near-significant increase in ebselen-treated mice in PFC ($p = 0.051$). Ebselen-treated mice differed from GLS1 Hets, in showing a higher ratio in all regions except CB, although not statistically significant.

3.5. Whole brain effects

We analyzed whole brain effects from the average of the individual measurements taken from the regions of interest (Fig. 5 and Supplemental Table for Fig. 5). Whole brain Glu concentrations (left panel) did not differ between groups; average Gln content appeared higher in GLS1 Hets compared to WT, although not statistically significant. Ebselen-treated mice differed from GLS1 Hets, in showing significant increases in GABA concentrations compared to GLS1 Hets ($p = 0.001$). GLS activity (right panel), measured as the ratio of 2-^{13}C-acetate labeled Glu-C4 to Gln-C4, was significantly lower in GLS1 Hets compared to WT ($p = 0.018$). Ebselen-treated mice differed significantly from GLS1 Hets ($p = 0.018$).

4. Discussion

In a regional *ex vivo* MRS study, we found that mice with a genetic heterozygous reduction in *Gls1* had diminished GLS activity, predominantly in the hippocampus, without overall changes in Gln, Glu or

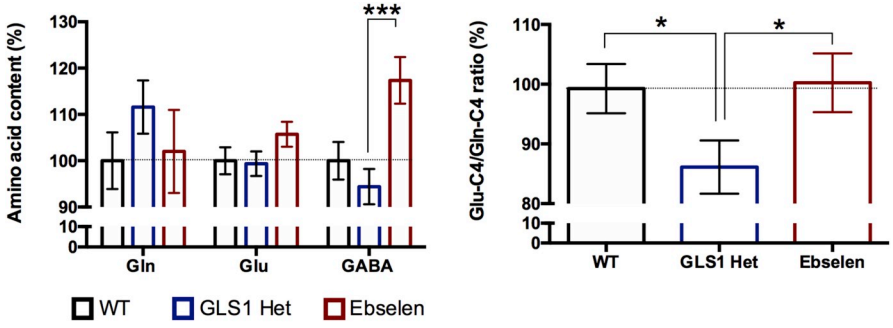

Fig. 5. Whole brain determinations of amino acid content and GLS activity, calculated from the average of the sampled regions, expressed as a percent of WT. Left panel shows ^{1}H content. There were no significant differences in Glu or Gln content; GABA showed overall differences in ebselen-treated mice. Right panel shows the ratio of [2–^{13}C]-acetate-enriched Glu-C4 to Gln-C4 at 15 min, as a measure of GLS activity. In GLS1 Het mice, the ratio was reduced (compared both to WT and ebselen-treated), while ebselen-treated mice did not differ from WT. *p < 0.05; ***p < 0.001.

GABA content. In contrast, putative pharmacological inhibition with ebselen did not affect GLS activity, had no impact on overall Gln or Glu content, but did increase GABA content. GLS1 Hets differed significantly from ebselen-treated mice in GLS activity, in line with more recent evidence that ebselen is not a potent GLS inhibitor (Zhu et al., 2017).

We found about a 15% reduction in GLS activity overall and about a 30% reduction in the hippocampus of GLS1 Hets, measured as a decrease in the ^{13}C-Glu-C4/^{13}C-Gln-C4 ratio after 15 min of ^{13}C-acetate infusion. Our results are in line with *in vitro* ^{13}C-Gln flux studies in hippocampal brain slices, where about a 30% reduction in GLS activity was seen in GLS1 Hets (El Hage et al., 2012). Effect sizes were similar, with a Cohen's d of 2.1 for *ex vivo* hippocampus in the present study compared to 3.5 for the previous *in vitro* HIP slice study (El Hage et al., 2012). The hippocampus appears to be more sensitive to GLS1 manipulations, which is in line with previous findings (Gaisler-Salomon et al., 2009a, 2012; Hazan and Gaisler-Salomon, 2014). It also validates the GLS1 Het model again as a GLS deficiency model. Differences in the Glu-C4/Gln-C4 ratio were driven mainly by Glu-C4 levels, as Gln-C4 was unchanged.

In awake rats, the rate of Glu neurotransmitter cycling is 0.5–0.6 μmol/g/min (Oz et al., 2004), which is ~24% of the rate of Gln hydrolysis by GLS measured in cortical homogenates *in vitro* under maximal rate (Vmax-like) conditions (2.1 μmol/g/min (Ward and Bradford, 1979). Assuming a comparable difference between the maximum activity of GLS Vmax and neurotransmitter flux in the control mice of our study, and considering the ~50% reduction in GLS protein in the Het mice, the enzyme activity present may be sufficient to maintain neurotransmitter rates in most brain regions except hippocampus, where GLS1 enzyme levels are apparently rate limiting, reflected by the lower flux measured as the ^{13}C-Glu/^{13}C-Gln ratio.

Ebselen did not reduce GLS activity, nor phenocopy the slight reductions in Glu-C4 content seen in GLS1 Hets, but did result in higher GABA-C2 than in GLS1 Hets. Indeed, ebselen would be expected to increase Glu content, as studies in synaptosomes show that the drug inhibits depolarization-evoked Glu release (Nogueira et al., 2002). Recently it was found that ebselen also inhibits GDH at the catalytic site (Jin et al., 2018), more potently than its GLS inhibitory action, since ebselen is not a very potent GLS inhibitor, with an IC_{50} of about 300 nM (Zhu et al., 2017). GDH catalyzes a reversible reaction between Glu and α-ketoglutarate so GDH inhibition could alter Glu levels. Ebselen also inhibits several other enzymes including thioredoxin reductase, glutathione peroxidase, lipoxygenases, nitric oxide synthase, NADPH oxidases, protein kinase C, H^+/K^+-ATPase, lactate dehydrogenase, and quiescin sulfhydryl oxidase (Haddad et al., 2002), pointing to multiple potential biological effects (Yu et al., 2017).

GABA content showed about a 20% overall increase in ebselen-treated mice, without regional differences. GABA is formed by GAD from Glu (Petroff, 2002). Establishing decreases in Glu and therefore excitatory drive, could be countered by reductions in GABA to maintain an excitatory/inhibitory balance; however, we did not see this compensation in GLS1 Hets. We did find that GABA-C2 levels differed between GLS1 Hets and ebselen-treated mice. This is partly in accordance with the current findings for endogenous Glu levels and the notion that GAD activity, and thus GABA synthesis, is possibly limited by the availability of Glu (Martin and Rimvall, 1993). Differences between the genetic reduction and putative pharmacological inhibition could also be due to the different temporal domains of the interventions.

The reduction in GLS activity, mainly in the hippocampus of GLS1 Hets phenocopies the reduction in cerebral blood volume (CBV) seen in the mice (Gaisler-Salomon et al., 2009a). CBV is a measure of vascular demand, which would decrease in response to lower energy metabolism, as it has been correlated to glucose uptake in localizing brain dysfunction (González et al., 1995). GLS deficiency was expected to slow Glu cycling, as seen in the diminished flux through GLS, and thus energy metabolism. Therefore it is of interest that the largest effect seen in the present MRS data is in the hippocampus, which corresponds with the CBV data showing hippocampal hypoactivity in GLS1 Hets (Gaisler-Salomon et al., 2009b). These convergent data point to distinct hippocampal effects and have clinical potential for biomarker discovery.

Various rodent models have been studied in regard to increased endogenous Glu levels with MK801 (Kosten et al., 2016; Wyckhuys et al., 2013), ketamine (Kosten et al., 2018; Sandiego et al., 2013) or other pharmacological challenges, as well as some rodent models in which Glu is decreased (Zimmer et al., 2015). GLUD1 transgenic mice, with increased activity of GDH in neurons resulting in elevated Glu levels have increased synaptic Glu release and later onset neurodegeneration (Michaelis et al., 2011). Mice with GLUD1 deficiency, predominantly in glial cells, also show increased Glu levels, and increased hippocampal activity, aligned with increased hippocampal Glu in patients at high risk of schizophrenia, and with schizophrenia (Lander et al., 2018). These rodent models variously affect Glu levels, creating difficulties in extrapolating findings between studies, motivating the present comparison of the genetic reduction in GLS1 Hets to pharmacologic inhibition with ebselen.

5. Conclusions

The current study reveals that acute administration of ebselen as a putative GLS inhibitor is not a means to inhibit GLS *in vivo* as achieved by the genetic manipulation. Other GLS inhibitors, though most recognized compounds lack blood-brain-barrier permeability or potency, should be tested to conclude whether pharmacologic manipulation of GLS would be a suitable alternative to genetic modification.

As a future direction, this approach identifies a molecular imaging strategy for testing target engagement for putative Glu modulators, comparing genetic and pharmacological reductions. It will be important to add comparison to global inducible reductions (Mingote et al., 2016) to align genetic and pharmacological strategies in adulthood in order to test whether adult inhibition of GLS can engender schizophrenia resilience and thus motivate therapeutic trials of GLS inhibition as a pharmacotherapy for schizophrenia.

Acknowledgements

This work was funded in part by *Fonds voor Wetenschappelijk Onderzoek - Vlaanderen* grant V4.228.16N, Yale Center for Clinical Investigation pilot support and NIH grant MH087758. We are grateful to Peter Dixon of MRRC, Yale University for help with brain extractions, to Xiaoxian Ma of MRRC, Yale University for assistance with animal preparation, to Bei Wang of MRRC, Yale University for animal care and preparation for infusions and to Johan Van Audekerke of Bio Imaging Lab, Antwerp University for help with data analysis.

Appendix A. Supplementary data

Supplementary data to this article can be found online at https://doi.org/10.1016/j.neuint.2019.104508.

References

Azad, G.K., Singh, V., Mandal, P., Singh, P., Golla, U., Baranwal, S., Chauhan, S., Tomar, R.S., 2014. Ebselen induces reactive oxygen species (ROS)-mediated cytotoxicity in *Saccharomyces cerevisiae* with inhibition of glutamate dehydrogenase being a target. FEBS Open Bio 4, 77–89. https://doi.org/10.1016/j.fob.2014.01.002.

Cabungcal, J.-H., Counotte, D.S., Lewis, E.M., Tejeda, H.A., Piantadosi, P., Pollock, C., Calhoon, G.G., Sullivan, E.M., Presgraves, E., Kil, J., Hong, L.E., Cuenod, M., Do, K.Q., O'Donnell, P., 2014. Juvenile antioxidant treatment prevents adult deficits in a developmental model of schizophrenia. Neuron 83, 1073–1084. https://doi.org/10.1016/j.neuron.2014.07.028.

Chowdhury, G.M.I., Patel, A.B., Mason, G.F., Rothman, D.L., Behar, K.L., 2007. Glutamatergic and GABAergic neurotransmitter cycling and energy metabolism in rat cerebral cortex during postnatal development. J. Cereb. Blood Flow Metab. 27, 1895–1907. https://doi.org/10.1038/sj.jcbfm.9600490.

Curthoys, N.P., Watford, M., 1995. Regulation of glutaminase activity and glutamine metabolism. Annu. Rev. Nutr. 15, 133–159. https://doi.org/10.1146/annurev.nu.15.

070195.001025.
de Graaf, R.A., Chowdhury, G.M.I., Brown, P.B., Rothman, D.L., Behar, K.L., 2009. In situ3D magnetic resonance metabolic imaging of microwave-irradiated rodent brain: a new tool for metabolomics research. J. Neurochem. 109, 494–501. https://doi.org/10.1111/j.1471-4159.2009.05967.x.
El Hage, M., Masson, J., Conjard-Duplany, A., Ferrier, B., Baverel, G., Martin, G., 2012. Brain slices from glutaminase-deficient mice metabolize less glutamine: a cellular metabolomic study with carbon 13 NMR. J. Cereb. Blood Flow Metab. 32, 816–824. https://doi.org/10.1038/jcbfm.2012.22.
Gaisler-Salomon, I., Miller, G.M., Chuhma, N., Lee, S., Zhang, H., Ghoddoussi, F., Lewandowski, N., Fairhurst, S., Wang, Y., Conjard-Duplany, A., Masson, J., Balsam, P., Hen, R., Arancio, O., Galloway, M.P., Moore, H.M., Small, S.A., Rayport, S., 2009a. Glutaminase-deficient mice display hippocampal hypoactivity, insensitivity to pro-psychotic drugs and potentiated latent inhibition: relevance to schizophrenia. Neuropsychopharmacology 34, 2305–2322. https://doi.org/10.1038/npp.2009.58.
Gaisler-Salomon, I., Schobel, S.A., Small, S.A., Rayport, S., 2009b. How high-resolution basal-state functional imaging can guide the development of new pharmacotherapies for schizophrenia. Schizophr. Bull. 35, 1037–1044. https://doi.org/10.1093/schbul/sbp114.
Gaisler-Salomon, I., Wang, Y., Chuhma, N., Zhang, H., Golumbic, Y.N., Mihali, A., Arancio, O., Sibille, E., Rayport, S., 2012. Synaptic underpinnings of altered hippocampal function in glutaminase-deficient mice during maturation. Hippocampus 22, 1027–1039. https://doi.org/10.1002/hipo.22014.
González, R.G., Fischman, A.J., Guimaraes, A.R., Carr, C.A., Stern, C.E., Halpern, E.F., Growdon, J.H., Rosen, B.R., 1995. Functional MR in the evaluation of dementia: correlation of abnormal dynamic cerebral blood volume measurements with changes in cerebral metabolism on positron emission tomography with fludeoxyglucose F 18. AJNR Am J Neuroradiol 16, 1763–1770.
Haddad, E.-B., McCluskie, K., Birrell, M.A., Dabrowski, D., Pecoraro, M., Underwood, S., Chen, B., De Sanctis, G.T., Webber, S.E., Foster, M.L., Belvisi, M.G., 2002. Differential effects of ebselen on neutrophil recruitment, chemokine, and inflammatory mediator expression in a rat model of lipopolysaccharide-induced pulmonary inflammation. J. Immunol. 169, 974–982.
Hazan, L., Gaisler-Salomon, I., 2014. Glutaminase 1 heterozygous mice show enhanced trace fear conditioning and Arc/Arg3.1 expression in hippocampus and cingulate cortex. Eur. Neuropsychopharmacol. 24, 1916–1924. https://doi.org/10.1016/j.euroneuro.2014.10.003.
Heffetz-Giterman, L., Lander, S.S., Cohen, R., Gross, A., Gaisler-Salomon, I., 2018. The glutaminase inhibitor ebselen prevents amphetamine sensitization in mice. Schizophr. Bull. 44 S202–S202.
Hertz, L., 2004. Intercellular metabolic compartmentation in the brain: past, present and future. Neurochem. Int. 45, 285–296. https://doi.org/10.1016/j.neuint.2003.08.016.
Jin, Y., Li, D., Lu, S., Zhao, H., Chen, Z., Hou, W., Ruan, B.H., 2018. Ebselen reversibly inhibits human glutamate dehydrogenase at the catalytic site. Assay Drug Dev. Technol. 16, 115–122. https://doi.org/10.1089/adt.2017.822.
Kosten, L., Verhaeghe, J., Verkerk, R., Thomae, D., De Picker, L., Wyffels, L., Van Eetveldt, A., Dedeurwaerdere, S., Stroobants, S., Staelens, S., 2016 Feb 28. Multiprobe molecular imaging of an NMDA receptor hypofunction rat model for glutamatergic dysfunction. Psychiatry Res. Neuroimaging 248, 1–11. https://doi.org/10.1016/j.pscychresns.2016.01.013.
Kosten, L., Verhaeghe, J., Wyffels, L., Stroobants, S., Staelens, S., 2018. Acute ketamine infusion in rat does not affect in vivo [^{11}C]ABP688 binding to metabotropic glutamate receptor subtype 5. Mol. Imaging 17, 1–5. https://doi.org/10.1177/1536012118788636.
Lander, S.S., Khan, U., Lewandowski, N., Chakraborty, D., Provenzano, F.A., Mingote, S., Chornyy, S., Frigerio, F., Maechler, P., Kaphzan, H., Small, S.A., Rayport, S., Gaisler-Salomon, I., 2018. Glutamate dehydrogenase-deficient mice display schizophrenia-like behavioral abnormalities and CA1-specific hippocampal dysfunction. Schizophr. Bull. https://doi.org/10.1093/schbul/sby011.
Leys, C., Ley, C., Klein, O., Bernard, P., Licata, L., 2013. Detecting outliers: do not use standard deviation around the mean, use absolute deviation around the median. J. Exp. Soc. Psychol. 49, 764–766. https://doi.org/10.1016/j.jesp.2013.03.013.
Martin, D.L., Rimvall, K., 1993. Regulation of gamma-aminobutyric acid synthesis in the brain. J. Neurochem. 60, 395–407.
Marx, M.-C., Billups, D., Billups, B., 2015. Maintaining the presynaptic glutamate supply for excitatory neurotransmission. J. Neurosci. Res. 93, 1031–1044. https://doi.org/10.1002/jnr.23561.
Masaki, C., Sharpley, A.L., Godlewska, B.R., Berrington, A., Hashimoto, T., Singh, N., Vasudevan, S.R., Emir, U.E., Churchill, G.C., Cowen, P.J., 2016. Effects of the potential lithium-mimetic, ebselen, on brain neurochemistry: a magnetic resonance spectroscopy study at 7 tesla. Psychopharmacology (Berl.) 233, 1097–1104. https://doi.org/10.1007/s00213-015-4189-2.
Masson, J., Darmon, M., Conjard, A., Chuhma, N., Ropert, N., Thoby-Brisson, M., Foutz, A.S., Parrot, S., Miller, G.M., Jorisch, R., Polan, J., Hamon, M., Hen, R., Rayport, S., 2006. Mice lacking brain/kidney phosphate-activated glutaminase have impaired glutamatergic synaptic transmission, altered breathing, disorganized goal-directed behavior and die shortly after birth. J. Neurosci. 26, 4660–4671. https://doi.org/10.1523/JNEUROSCI.4241-05.2006.
Michaelis, E.K., Wang, X., Pal, R., Bao, X., Hascup, K.N., Wang, Y., Wang, W.-T., Hui, D., Agbas, A., Choi, I.-Y., Belousov, A., Gerhardt, G.A., 2011. Neuronal Glud1 (glutamate dehydrogenase 1) over-expressing mice: increased glutamate formation and synaptic release, loss of synaptic activity, and adaptive changes in genomic expression. Neurochem. Int. 59, 473–481. https://doi.org/10.1016/j.neuint.2011.03.003.
Mihali, A., Subramani, S., Kaunitz, G., Rayport, S., Gaisler-Salomon, I., 2012. Modeling resilience to schizophrenia in genetically modified mice: a novel approach to drug discovery. Expert Rev. Neurother. 12, 785–799. https://doi.org/10.1586/ern.12.60.
Mingote, S., Masson, J., Gellman, C., Thomsen, G., Lin, C.-S., Merker, R., Gaisler-Salomon, I., Wang, Y., Ernst, R., Hen, R., Rayport, S., 2016. Genetic pharmacotherapy as an early CNS drug development strategy: testing glutaminase inhibition for schizophrenia treatment in adult mice. Front. Syst. Neurosci. 9, 1–12. https://doi.org/10.3389/fnsys.2015.00165.
Nogueira, C.W., Rotta, L.N., Zeni, G., Souza, D.O., Rocha, J.B.T., 2002. Exposure to ebselen changes glutamate uptake and release by rat brain synaptosomes. Neurochem. Res. 27, 283–288.
Oz, G., Berkich, D.A., Henry, P.-G., Xu, Y., LaNoue, K., Hutson, S.M., Gruetter, R., 2004. Neuroglial metabolism in the awake rat brain: CO_2 fixation increases with brain activity. J. Neurosci. 24, 11273–11279. https://doi.org/10.1523/JNEUROSCI.3564-04.2004.
Ozyigit, F., Kucuk, A., Akcer, S., Tosun, M., Kocak, F.E., Kocak, C., Kocak, A., Metineren, H., Genc, O., 2015. Different dose-dependent effects of ebselen in sciatic nerve ischemia-reperfusion injury in rats. Bosn. J. Basic Med. Sci. 15, 36–43.
Patel, A.B., de Graaf, R.A., Rothman, D.L., Behar, K.L., Mason, G.F., 2010. Evaluation of cerebral acetate transport and metabolic rates in the rat brain in vivo using ^{1}H-[^{13}C]-NMR. J. Cereb. Blood Flow Metab. 30, 1200–1213. https://doi.org/10.1038/jcbfm.2010.2.
Petroff, O.A.C., 2002. GABA and glutamate in the human brain. The Neuroscientist 8, 562–573. https://doi.org/10.1177/1073858402238515.
Rumping, L., Büttner, B., Maier, O., Rehmann, H., Lequin, M., Schlump, J.-U., Schmitt, B., Schiebergen-Bronkhorst, B., Prinsen, H.C.M.T., Losa, M., Fingerhut, R., Lemke, J.R., Zwartkruis, F.J.T., Houwen, R.H.J., Jans, J.J.M., Verhoeven-Duif, N.M., van Hasselt, P.M., Jamra, R., 2018. Identification of a loss-of-function mutation in the context of glutaminase deficiency and neonatal epileptic encephalopathy. JAMA Neurol. https://doi.org/10.1001/jamaneurol.2018.2941.
Sandiego, C.M., Nabulsi, N., Lin, S.-F., Labaree, D., Najafzadeh, S., Huang, Y., Cosgrove, K., Carson, R.E., 2013. Studies of the metabotropic glutamate receptor 5 radioligand [^{11}C]ABP688 with N-acetylcysteine challenge in rhesus monkeys. Synapse 67, 489–501. https://doi.org/10.1002/syn.21656.
Sibson, N.R., Dhankhar, A., Mason, G.F., Behar, K.L., Rothman, D.L., Shulman, R.G., 1997. *In vivo* ^{13}C NMR measurements of cerebral glutamine synthesis as evidence for glutamate-glutamine cycling. Proc. Natl. Acad. Sci. U.S.A. 94, 2699–2704.
Sies, H., 1993. Ebselen, a selenoorganic compound as glutathione peroxidase mimic. Free Radic. Biol. Med. 14, 313–323.
Singh, N., Halliday, A.C., Thomas, J.M., Kuznetsova, O.V., Baldwin, R., Woon, E.C.Y., Aley, P.K., Antoniadou, I., Sharp, T., Vasudevan, S.R., Churchill, G.C., 2013. A safe lithium mimetic for bipolar disorder. Nat. Commun. 4, 1332. https://doi.org/10.1038/ncomms2320.
Thomas, A.G., Rojas, C., Tanega, C., Shen, M., Simeonov, A., Boxer, M.B., Auld, D.S., Ferraris, D.V., Tsukamoto, T., Slusher, B.S., 2013. Kinetic characterization of ebselen, chelerythrine and apomorphine as glutaminase inhibitors. Biochem. Biophys. Res. Commun. 438, 243–248. https://doi.org/10.1016/j.bbrc.2013.06.110.
Ward, H.K., Bradford, H.F., 1979. Relative activities of glutamine synthetase and glutaminase in mammalian synaptosomes. J. Neurochem. 33, 339–342.
Wyckhuys, T., Verhaeghe, J., Wyffels, L., Langlois, X., Schmidt, M., Stroobants, S., Staelens, S., 2013. N-acetylcysteine- and MK-801-induced changes in glutamate levels do not affect *in vivo* binding of metabotropic glutamate 5 receptor radioligand ^{11}C-ABP688 in rat brain. J. Nucl. Med. https://doi.org/10.2967/jnumed.113.121608.
Yu, Y., Jin, Y., Zhou, J., Ruan, H., Zhao, H., Lu, S., Zhang, Y., Li, D., Ji, X., Ruan, B.H., 2017. Ebselen: mechanisms of glutamate dehydrogenase and glutaminase enzyme inhibition. ACS Chem. Biol. 12, 3003–3011. https://doi.org/10.1021/acschembio.7b00728.
Zhu, M., Fang, J., Zhang, J., Zhang, Z., Xie, J., Yu, Y., Ruan, J.J., Chen, Z., Hou, W., Yang, G., Su, W., Ruan, B.H., 2017. Biomolecular interaction assays identified dual inhibitors of glutaminase and glutamate dehydrogenase that disrupt mitochondrial function and prevent growth of cancer cells. Anal. Chem. 89, 1689–1696. https://doi.org/10.1021/acs.analchem.6b03849.
Zimmer, E.R., Parent, M.J., Leuzy, A., Aliaga, A., Aliaga, A., Moquin, L., S, Schirrmacher, E., Soucy, J.-P., Skelin, I., Gratton, A., Gauthier, S., Rosa-Neto, P., 2015. Imaging in vivo glutamate fluctuations with [^{11}C]ABP688: a GLT-1 challenge with ceftriaxone. J. Cereb. Blood Flow Metab. https://doi.org/10.1038/jcbfm.2015.35.